

⁸Gutmark, E., Wilson, K. J., Schadow, K. C., Parr, T. P., and Hanson-Parr, D. M., "Combustion Enhancement in Supersonic Coaxial Flows," AIAA Paper 89-2788, 1989.

⁹Schadow, K. C., and Gutmark, E., "Review of Passive Shear Flow Control Research for Improved Subsonic and Supersonic Combustion," AIAA Paper 89-2786, 1989.

¹⁰Tillman, T. G., Patrick, W. P., and Paterson, R. W., "Enhanced Mixing of Two Coaxial High Speed Streams," *Journal of Propulsion and Power*, Vol. 7, No. 6, 1991, pp. 1006–1014.

¹¹Narayanan, A. K., and Damodaran, K. A., "Experimental Studies on Mixing of Two Coaxial High Speed Streams," *Journal of Propulsion and Power*, Vol. 10, No. 1, 1994, pp. 62–68.

¹²Narayanan, A. K., and Damodaran, K. A., "Preliminary Investigations on Improving Air Augmented Rocket Performance," *Journal of Propulsion and Power*, Vol. 10, No. 3, 1994, pp. 432–434.

¹³Rajamanohar, D., Kurian, J., and Damodaran, K. A., "Experimental Studies on the Effect of Primary Nozzle Geometry for High Speed Mixing and in Supersonic Ejectors," *Proceedings of the 2nd National Conference on Airbreathing Engines and Aerospace Propulsion*, ISRO, Trivandrum, India, 1994, pp. 110–118.

¹⁴Chinzei, N., Komuro, T., Kudou, K., Murakami, A., Jani, K., Masuya, G., and Wakamatsu, Y., "Effects of Injector Geometry on Scramjet Combustor Performance," *Journal of Propulsion and Power*, Vol. 9, No. 1, 1993, pp. 146–152.

Numerical Simulations of Unsteady Transonic Flow in Turbomachines

Daniel J. Dorney*

Western Michigan University,
Kalamazoo, Michigan 49008

and

Roger L. Davis†

United Technologies Research Center,
East Hartford, Connecticut 06108

Nomenclature

- C_f = skin friction coefficient
 p = unsteady pressure
 q = velocity magnitude
 v_g = vortical gust amplitude
 β = flow angle
 θ = momentum thickness
 ρ = density
 ϕ = phase angle
 ω = reduced temporal frequency

Subscripts

- chd = chordwise direction
 1 = inlet quantity

Superscripts

- + = upper surface of blade
 - = lower surface of blade

Presented as Paper 94-2833 at the AIAA/ASME/SAE/ASEE 30th Joint Propulsion Conference, Indianapolis, IN, June 27–29, 1994; received July 22, 1995; revision received Nov. 1, 1995; accepted for publication Nov. 7, 1995. Copyright © 1995 by the American Institute of Aeronautics and Astronautics, Inc. All rights reserved.

*Assistant Professor, Department of Mechanical and Aeronautical Engineering. Senior Member AIAA.

†Senior Principal Engineer. Senior Member AIAA.

Introduction

THE need for improved durability, reduced noise levels, and increased performance has motivated engineers to assess the effects of flow unsteadiness on the aerodynamic phenomena present in axial-flow turbomachines. For coupled systems of rotating and stationary blade rows, the relative motions between adjacent rows give rise to high-frequency unsteady aerodynamic excitations that can reduce performance and generate discrete-tone noise. Two categories of numerical procedures have been developed for determining the effects of relative motion between adjacent blade rows. In the first category of procedures, incoming wakes are specified at the inlet of isolated blade rows.¹ In these methods the wakes are usually assumed to be parallel, with uniform pressure and a prescribed total enthalpy and/or velocity variation. In the second category of analyses, both blade rows are modeled and the relative position of one blade row is varied to simulate blade motion.^{2,3} The work in this study utilizes the first category of numerical procedures.

In a recent study, unsteady inlet and exit boundary conditions were formulated and implemented into an implicit two-dimensional Navier–Stokes procedure.⁴ The inlet and exit boundary conditions were designed to be time-accurate and nonreflecting. In addition, the boundary conditions were constructed to allow the specification of entropic, vortical, and acoustic excitations at the inlet, and acoustic excitations at the exit of the computational domain. The focus of the current investigation is to study the unsteady response of a transonic compressor cascade to inlet vortical gusts.

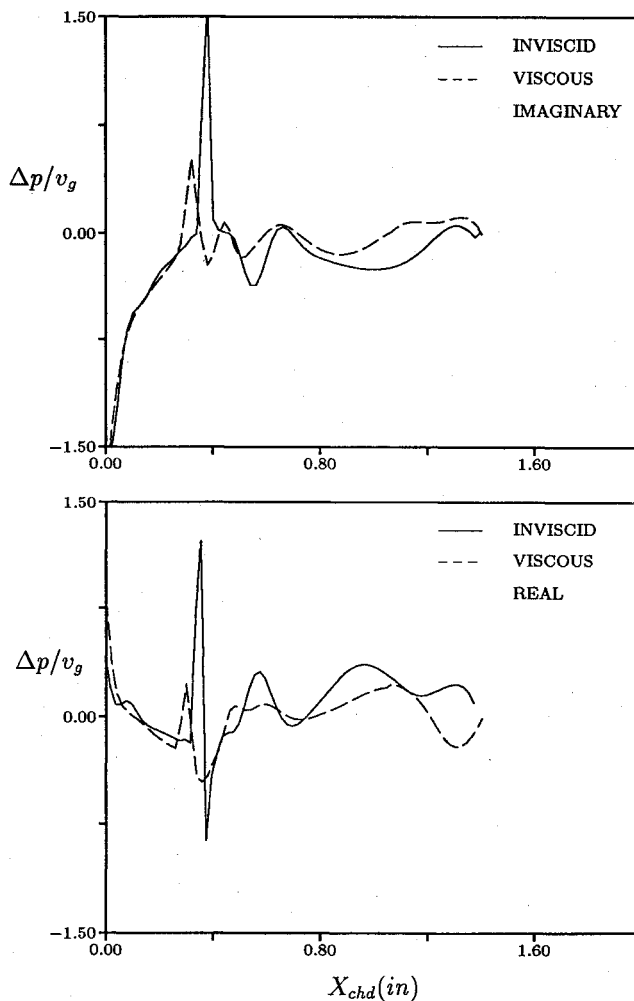


Fig. 1 Real and imaginary components of the unsteady pressure difference.

Solution Algorithm

The implicit numerical procedure used in this study consists of a time-marching finite difference scheme.⁴ The procedure is second-order temporally accurate and third-order spatially accurate. The inviscid fluxes are discretized using an upwind-biased scheme, while the viscous fluxes are discretized using standard central differences. An alternating direction, approximate-factorization technique is used to compute the time-rate changes in the primary variables. Newton subiterations are used at each global time step to increase stability and reduce

linearization errors. For unsteady simulations, two Newton subiterations are typically performed at each time step.

Numerical Results

To investigate the response of a blade row to unsteady vortical excitations in transonic flow, inviscid, and viscous simulations have been performed for the tenth standard configuration cascade.⁵ The compressor cascade has a stagger angle Ω of 45 deg, a pitchwise gap G of 1.41, operates at an inlet Mach number of 0.80, and an inlet flow angle of $\beta_1 = 58$ deg. The

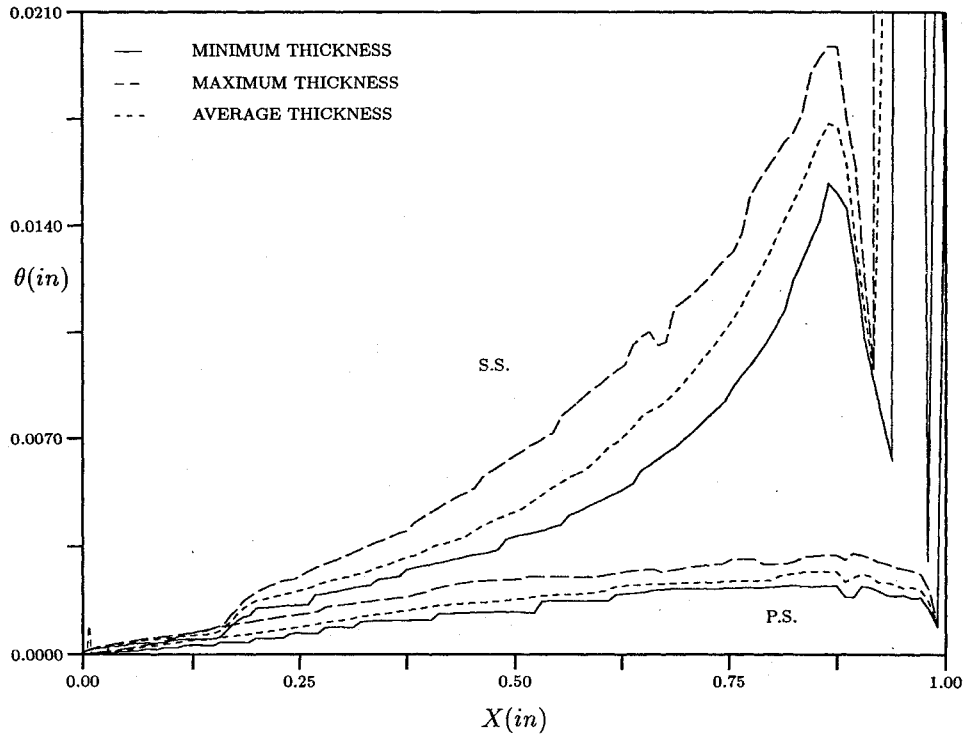


Fig. 2 Momentum thickness envelope.

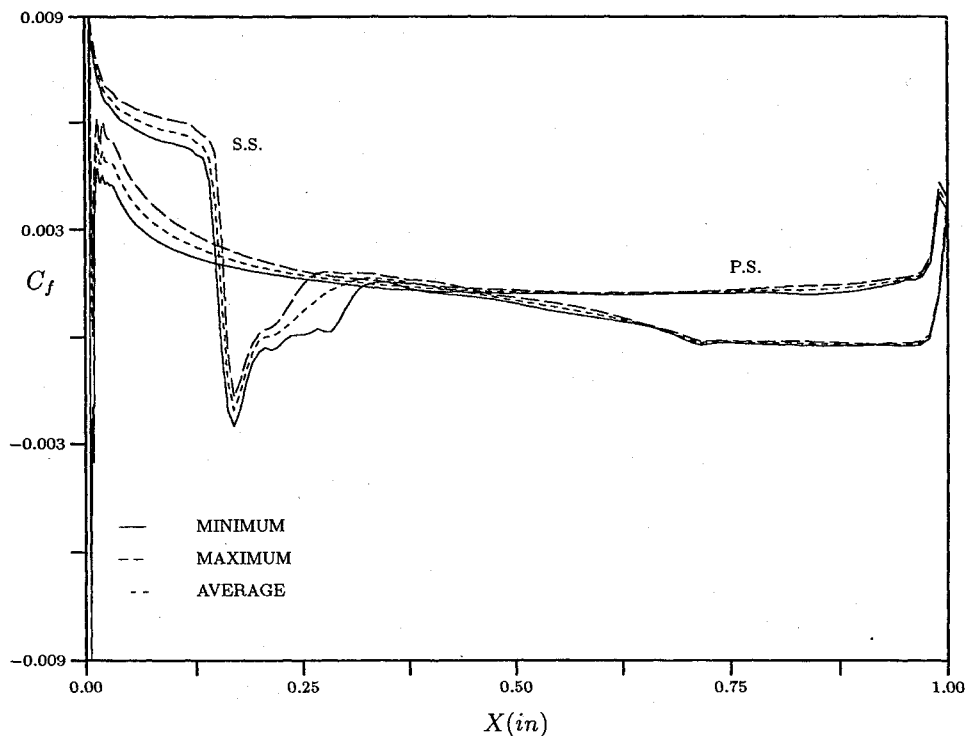


Fig. 3 Skin friction coefficient envelope.

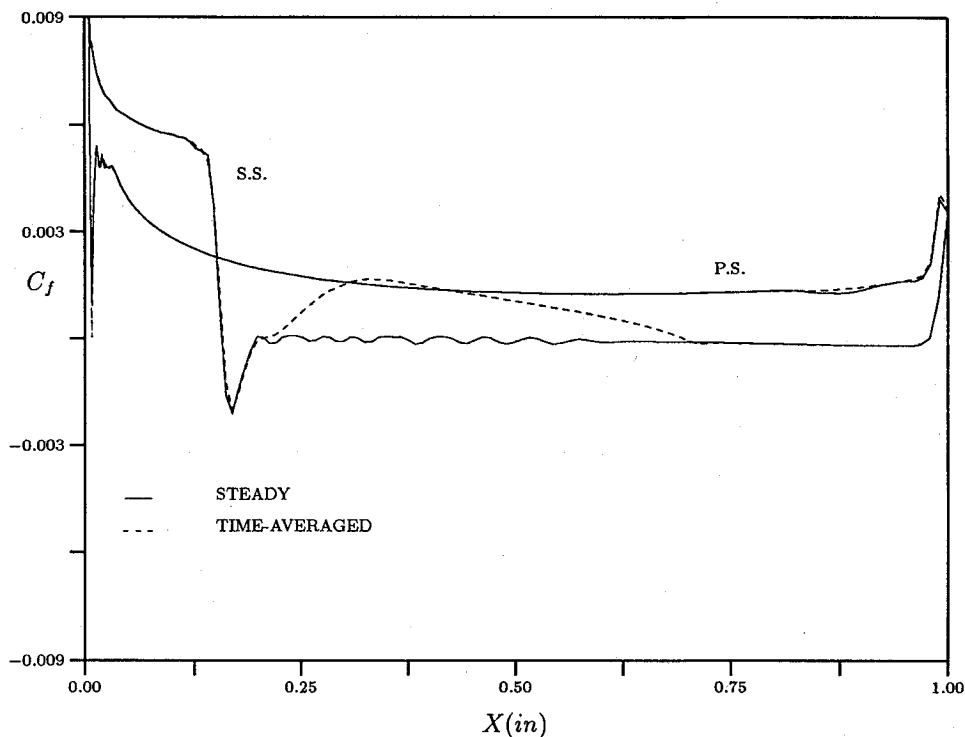


Fig. 4 Steady and time-averaged skin friction distributions.

mass flow was held constant between the inviscid and viscous simulations by adjusting the average exit static pressure. In the viscous simulations, the Reynolds number, based on the inlet freestream conditions and the blade axial chord, was set at $Re = 7.09 \times 10^5$. A zero heat flux condition was specified at the blade surface. Transition was assumed to occur at the leading edge of each blade. In the unsteady flow simulations, vortical gusts at ω of 10 and an interblade phase angle σ of -2π were introduced at the inlet boundary. The gust amplitude was set equal to 5% of the steady inlet flow velocity $v_g = 0.05q_1$.

The computational grid topology used in the inviscid simulation contained a total of 13,601 grid points, while the computational grid used in the viscous simulation contained 21,591 grid points. In the viscous simulation, the average value of y^+ , the nondimensional distance of the first grid point above the surface, was equal to 0.50. The inviscid simulation required 0.00019 s of CPU time per grid point per iteration (with two Newton subiterations) on a DEC 3000-400 workstation and the viscous simulation required 0.00026 s of CPU time per grid point per iteration. For the unsteady simulations, eight periods at 2000 iterations per period were necessary to achieve a time-periodic solution.

The unsteady pressure response of the blade row to the passing wakes is described using a complex representation. The magnitude and phase of the unsteady pressure response at any location are given by $p = \{[Re(p)]^2 + [Im(p)]^2\}^{1/2}$ and $\phi = \tan^{-1}[Im(p)/Re(p)]$, where the phase angle is measured relative to the phase of the excitation. The real and imaginary components of the first harmonic of the unsteady pressure difference distributions along the blade surface are shown in Fig. 1. The unsteady pressure difference is defined as

$$\Delta p(x)/v_g = [p^-(x_{chd}, t) - p^+(x_{chd}, t)]/(\rho_1 q_1^2 v_g) \quad (1)$$

where x_{chd} is the distance along the blade chord, ρ_1 is the steady inlet density, and q_1 is the steady inlet velocity. In presenting the numerical results, the pressure difference is scaled by the amplitude of the unsteady excitation v_g . The relatively high frequency of the vortical distortion is seen to cause large variations in the inviscid unsteady pressure difference along the

surface of the blade. Figure 1 suggests that the fluid viscosity acts to damp some of the large spatial fluctuations in the unsteady pressure. The general trends predicted in the inviscid and viscous analyses are similar, but changes in the location and strength of the shock because of the viscous boundary layer are evident.

In an effort to study the unsteady nature of the viscous flow, the unsteady boundary-layer momentum thickness and skin friction coefficient distributions were recorded and interrogated. Figure 2 shows the unsteady momentum thickness envelope, which is comprised of the maximum, minimum, and time-averaged values over one wake-passing cycle. The momentum thickness shows large excursions about the time-averaged values, but behaves in a linear manner (i.e., the time-averaged and steady distributions are similar). In Fig. 3, which shows the unsteady skin-friction-coefficient envelope, the location of the shock wave is marked by a significant reduction in the skin friction. The skin friction varies mainly over the first 25% of the pressure surface, while larger variations are noticeable along the suction surface up to the separation point. Figure 3 also suggests there is flow separation near the base of the shock. The location of the downstream flow separation point in the unsteady simulation is not affected by the periodic unsteadiness. Comparing the steady and time-averaged skin friction distributions reveals nonlinear behavior downstream of the shock (see Fig. 4). In the steady simulation the flow is intermittently separated from the shock to the trailing edge, while the time-averaged flow solution indicates that the flow reattaches downstream of the shock and does not separate again until approximately 70% of the axial chord.

Conclusions

A two-dimensional Navier-Stokes analysis has been used to study unsteady transonic flow through a compressor cascade, subject to inlet vortical disturbances. The predicted inviscid unsteady pressure distributions exhibit large spatial fluctuations because of the high frequency of the vortical disturbance, while the viscous results indicate that the fluid viscosity acts to dampen out some of the unsteadiness near the blade surface. Investigation of the viscous-layer quantities re-

vealed that the momentum thickness responds in a linear manner to the passing wakes, but the skin friction distribution exhibits significant nonlinear behavior.

References

- ¹Giles, M. B., "Nonreflecting Boundary Conditions for Euler Equation Calculations," *AIAA Journal*, Vol. 28, No. 12, 1990, pp. 2050–2058.
- ²Rai, M. M., "Three-Dimensional Navier-Stokes Simulations of Turbine Rotor-Stator Interaction," *Journal of Propulsion and Power*, Vol. 5, No. 3, 1989, pp. 307–319.
- ³Rao, K. V., Delaney, R. A., and Dunn, M. G., "Vane-Blade Interaction in a Transonic Turbine Part I—Aerodynamics," *Journal of Propulsion and Power*, Vol. 10, No. 3, 1994, pp. 305–311.
- ⁴Dorney, D. J., and Verdon, J. M., "Numerical Simulations of Unsteady Cascade Flows," *Journal of Turbomachinery*, Vol. 116, Oct. 1994, pp. 665–675.
- ⁵Verdon, J. M., Barnett, M., Ayer, T. C., and Montgomery, M. D., "Development of Unsteady Aerodynamic Analyses and Codes for Turbomachinery Aeroelastic and Aeroacoustic Design Predictions," NAS3-25425 Interim Rept., 1993.

Estimation of Mixing of High-Speed Streams

R. Ramesh Kumar* and Job Kurian†

Indian Institute of Technology, Madras 600 036, India

Nomenclature

| | |
|----------|---|
| D | = diameter of mixing tube |
| E_Q | = basic unit based on Q |
| G | = mass flow flux |
| K_a | = factor of uniformity of total pressure between axes |
| K_r | = factor of radial uniformity of total pressure |
| M | = Mach number |
| MF | = momentum flux |
| P | = total pressure |
| p | = static pressure |
| Q | = physical quantity |
| r | = radial coordinate |
| v | = velocity |
| x | = axial coordinate |
| γ | = ratio of specific heats |
| η | = mixing parameter |
| ρ | = density |

Subscripts

| | |
|--------|--|
| A, B | = measurement locations in a plane perpendicular to the flow direction |
| m | = mean value along radial direction |

Introduction

ESTIMATION of experimental mixing performance is critical to assess the various passive supersonic mixing enhancement devices^{1–3} and ejector systems.^{4,5} The problem gets further compounded in the mixing of flows with the same inlet total temperature, and using the same working medium, as stream identification is difficult. Decay of centerline properties and spreading rates of jets have been used by many investi-

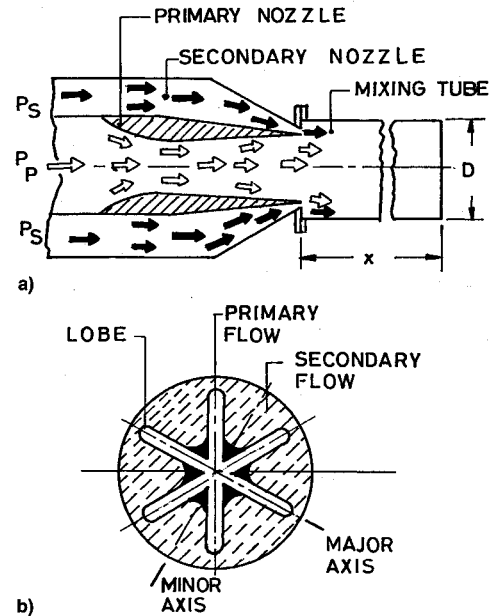


Fig. 1 Flow configuration: a) schematic and b) end view of a radially lobed nozzle.

gators^{1,3} as indicators of mixing performance. However, as noted by Naughton et al.⁶ these parameters are more representative of the penetration of the jet into the surrounding medium. Mixing parameters have been based on momentum flux,^{2,5} as it remains constant across shocks (from inviscid, nonfrictional one-dimensional flow analysis). However, a parametric study is not available to justify this choice. Though uniformity of mean flow profiles has been used by many investigators to evaluate mixing performance, Dimotakis⁷ suggested that an increasingly uniform distribution of mean flow quantities is not the ultimate check for molecular scale mixing essential for combustion. However, gas sampling measurements of Gutmark et al.⁸ suggest that pressure measurements can be used to make reasonable estimates of mixing rates.

This Note suggests a simple method to obtain a physically meaningful estimate of mixing performance in the context of interacting coaxial streams (see Fig. 1a) using typical discrete experimental data. As efficient mixing of the coaxial streams with different inlet conditions involves exchange of properties until the gradients are reduced, the emphasis is on a parameter that amplifies any existing difference (to highlight the extent of the lack of mixing) in physical quantities in a given flow cross section.

The extent of mixing of flows is assessed at planes perpendicular to the mean flow direction. First the basic unit used in η is developed; later η is formulated for an axisymmetric and a nonaxisymmetric flow.

Results and Discussion

Formulation of Basic Unit

If the basic unit E_Q of η uses a physical quantity, the difference $Q_B - Q_A$ should reduce as the flow becomes increasingly mixed. Because of the dissipative nature of efficient mixing devices, normalization of $(Q_B - Q_A)$ in the basic unit is done with local quantities. Because of its greater amplification of the difference, Q_A is preferred over the average of Q_A and Q_B as the normalizing factor. To incorporate the effects of pressure, density, and velocity on the mixing process, the physical quantities considered were 1) momentum flux $p + \rho v^2$, 2) mass flow flux ρv , and 3) total pressure. Again, the physical quantity that yields the largest value for the basic unit is chosen.

Based on the measurements at locations A and B , without loss of generality, it can be assumed that $p_B = p_A + \Delta p$ and

Received April 27, 1995; revision received June 14, 1995; accepted for publication Aug. 30, 1995. Copyright © 1995 by the American Institute of Aeronautics and Astronautics, Inc. All rights reserved.

*Research Associate, Department of Aerospace Engineering.

†Associate Professor, Department of Aerospace Engineering.